USA-JAPAN Symposium on Flexible Automation
July 18 - 20, 1988, Minneapolis, Minnesota

# Design and Control of a Statically Balanced Direct Drive Manipulator

**H. Kazerooni**
**S. Kim**

**The productivity Center and the Mechanical Engineering Department**
**University of Minnesota**
**Minneapolis, MN 55455**

## ABSTRACT

A practical architecture, using a four-bar-linkage, is considered for the University of Minnesota direct drive robot [14]. This statically- balanced direct drive robot has been constructed for stability analysis of the robot in constrained manipulation [8, 10 -14]. As a result of the elimination of the gravity forces (without any counter weights), smaller actuators and consequently smaller amplifiers were chosen. The motors yield acceleration of 5g at the end point without overheating. High torque, low speed, brush-less AC synchronous motors are used to power the robot. Graphite-epoxy composite material is used for the construction of the robot links. A 4-node parallel processor has been used to control the robot. The dynamic tracking accuracy -with the feedforward torque method as a control law- has been derived experimentally.

Figure 1: University of Minnesota Direct Drive Arm .

## INTRODUCTION

The work presented here is on the design and control of the Minnesota direct drive robot. This robot is statically balanced and uses a four bar link mechanism to compensate for some of the drawbacks of serial type [2] and parallelogram type [4] direct drive robots.

Conventional robot manipulators with electric servomotors are driven through speed reducers. Although speed reducers generate large torque, they usually introduce backlash, compliance, cogging, and friction into the systems. Studies on several industrial robots indicate that the powertrain compliance forms over 80% of total arm compliance [7,21]. Also the friction torque generated by reducer is about 25% of the total required torque in any maneuver. [6].

Several attempts have been made to improve the manipulator dynamic behavior. Asada and Kanade [2] designed a serial type direct drive arm in which the actuators were directly coupled to links without any transmission mechanism. The elimination of the transmission mechanism improved the robot performance, however large motors were needed to drive the robot. Asada and Youcef-Toumi [4] studied a direct drive arm with a parallelogram mechanism to eliminate the problems associated with serial type robots. A direct drive arm with a counterweight was designed by Takase et al. [22] in order to eliminate the gravity effect at three major joints. Another direct drive arm, designed by Kuwahara et al. [16] to reduce the effect of gravity using a four bar link for the forearm, and a special spring for the upper arm. The counterweight provides the system balance for all possible positions, however it increases the total inertia of the robot arm. The spring balancing will not perfectly balance the system either [18].

In this research, a statically balanced direct drive arm is designed to achieve improved dynamic behavior. As a result of the elimination of the gravity forces (without any counter weights), smaller actuators and consequently smaller amplifiers were chosen. The motors yield acceleration of 5g at the end point without overheating.

## ARCHITECTURE

The architecture of this arm is such that the gravity term is completely eliminated from the dynamic equations. This balanced mechanism is designed without adding any extra counterbalance weights. The new features of this new design are as follows:

I. Since the motors are never affected by gravity, the static load will be zero. Hence no overheating results in the system in the static case.
II. Because of the elimination of the gravity terms, smaller motors with less stall torque (and consequently smaller amplifiers) have been chosen for a desired acceleration.
III. Because of the lack of gravity terms, higher accuracy can be achieved. This is true because the links have steady deflection due to constant gravity effect. This gives better accuracy and repeatability for fine manipulation tasks.
IV. As depicted in Figure 3, the architecture of this robot allows for a "large" workspace. The horizontal workspace ( radius = 80 cm ) of this robot is quite attractive from the stand point of manufacturing tasks such as assembly and deburring.
V. Graphite-epoxy composite material is used for the construction of the robot links. This robot is light ( 60 kg ) and can be mounted on an autonomous vehicle. The pay load without losing precision is 2 kg.

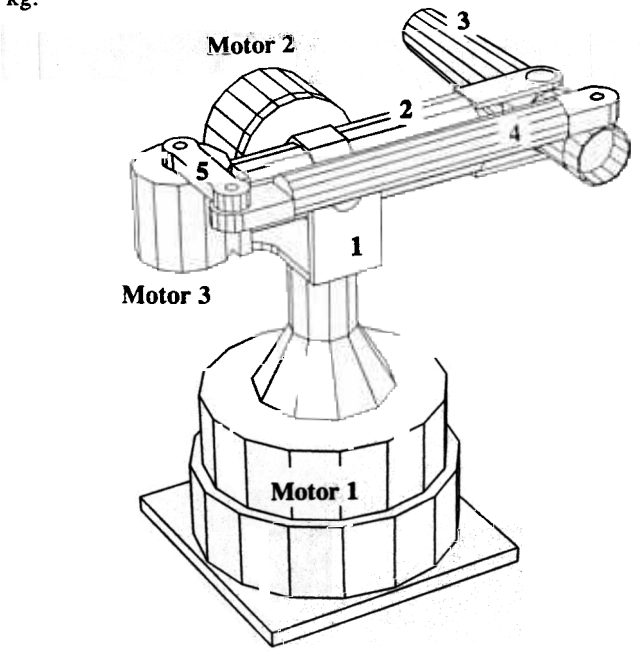


Figure 2: Schematic of University of Minnesota Arm

Figure 2 shows the schematic diagram of the University of Minnesota direct drive arm. The arm has three degrees of freedom, all of which are articulated drive joints. Motor 1 powers the system about a vertical axis. Motor 2 pitches the entire four-bar-linkage while motor 3 is used to power the four-bar-linkage. Link 2 is directly connected to the shaft of motor 2. Figure 3 shows the top view and side view of the robot. The coordinate frame $X_iY_iZ_i$ has been assigned to link i of the robot for i=1,2,..,5. The center of coordinate frame $X_1Y_1Z_1$ corresponding to link 1 is located at point O as shown in figure 3. The center of the inertial global coordinate frame $X_0Y_0Z_0$ is also located at point 0 (The global coordinate frame is not shown in the figures). The joint angles are represented by $\theta_1$, $\theta_2$, and $\theta_3$. $\theta_1$ represents the rotation of link 1; coordinate frame $X_1Y_1Z_1$ coincides on global coordinate frame $X_0Y_0Z_0$ when $\theta_1$=0. $\theta_2$ represents the pitch angle of the four-bar-linkage as shown in figure 3. $\theta_3$ represents the angle between link 2 and link 3. Shown are the conditions under which the gravity terms are eliminated from the dynamic equations.

Figure 4 shows the four-bar-linkage with assigned coordinate frames. By inspection the conditions under which the vector of gravity passes through origin, O, for all possible values of $\theta_1$ and $\theta_3$ are given by equations (1) and (2).

$$[\, m_3\bar{x}_3 - m_4L_5 - m_5\bar{x}_5 \,] \sin\theta_3 = 0 \qquad (1)$$

$$g\,(mt_3 + m_5) - m_2\bar{x}_2 - m_3(L_2 - g) - m_4(\bar{x}_4 - g) - [\, m_3\bar{x}_3 - m_4L_5 - m_5\bar{x}_5 \,] \cos\theta_3 = 0 \qquad (2)$$

where:
$m_i$, $L_i$ = mass and length of each link,
$\bar{x}_i$ = the distance of center of mass from the origin of each coordinate frame,
$mt_3$ = mass of motor 3.

Conditions (1) and (2) result in:

$$m_3\bar{x}_3 - m_4L_5 - m_5\bar{x}_5 = 0 \qquad (3)$$

$$g(mt_3 + m_5) - m_2\bar{x}_2 - m_3(L_2 - g) - m_4(\bar{x}_4 - g) = 0 \qquad (4)$$

If equations (3) and (4) are satisfied, then the center of gravity of the four-bar-linkage passes through point O for all the possible configurations of the arm. Note that the gravity force still passes through O even if the plane of the four-bar-linkage is tilted by motor 2 for all values of $\theta_2$.

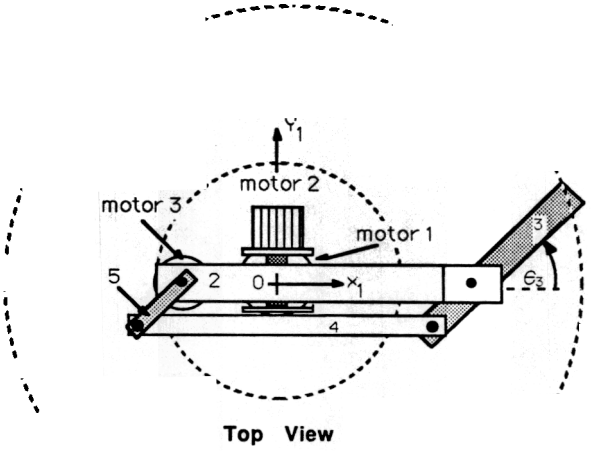


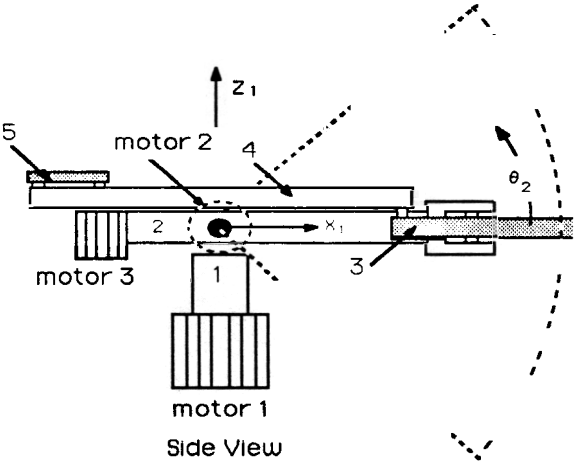


Figure 3: The side view and top view of the robot

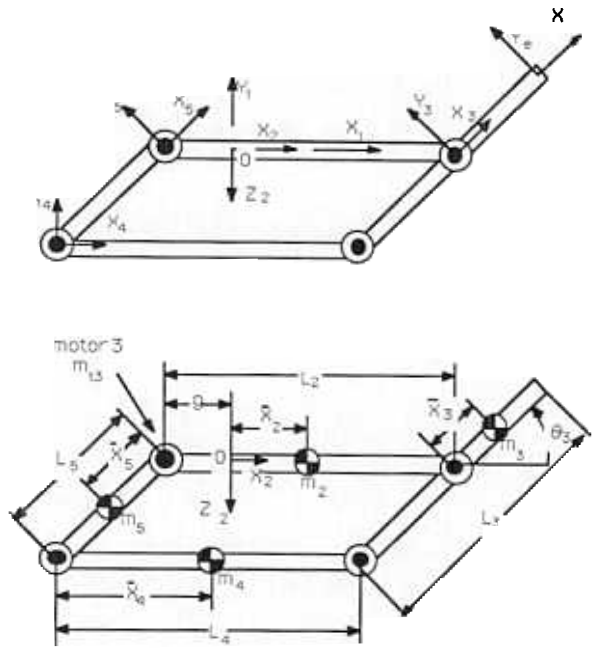


**Figure 4: Four bar link mechanism**

Since at low speeds, AC torque motors do not tend to cog, low speed, high torque, and brush-less AC synchronous motors have been chosen to power the robot. Each motor consists of a ring shaped stator and a ring shaped permanent magnet rotor with a large number of poles. The rotor is made of rare earth magnetic material (Neodymium) bonded to a low carbon steel yoke with structural adhesive. The stator of the motor (with winding) is fixed to the housing for heat dissipation. To develop wide bandwidth (high speed) closed control for the robot, Graphite-expoxy composite and AA7075T6 Materials were used to construct the links. The high structural stiffness and low density of the Graphite-expoxy composite result in high natural frequencies in the robot dynamics. The higher the natural frequencies are, the wider the bandwidth and consequently faster the closed loop system will be [9]. A strong bond between the composite parts and the aluminum parts was achieved using an epoxy adhesive (3M Epoxy Adhesive EC - 3569 B/A ). To minimize joint clearance and reduce bearing mass, Super Precision angular contact bearings (ABEC- 7, extremely light series 1900 ) were used.

## FORWARD KINEMATICS

The forward kinematic problem is to compute the position of the end point in the global coordinate frame $X_0Y_0Z_0$, given the joint angles, $\theta_1$, $\theta_2$, and $\theta_3$. The end point position of the robot relative to the global coordinate frame is characterized by $P_x$, $P_y$, and $P_z$ in the global coordinate frame $X_0Y_0Z_0$:

$$P_x = [C_1C_2C_3 - S_1S_3][L_3-L_5] + C_1C_2[L_2 - g] \quad (5)$$

$$P_y = [S_1C_2C_3 + C_1S_3][L_3-L_5] + S_1C_2[L_2 - g] \quad (6)$$

$$P_z = S_2[L_2 - g] + S_2C_3[L_3 - L_5] \quad (7)$$

where $S_i = \sin(\theta_i)$, and $C_i = \cos(\theta_i)$.

## INVERSE KINEMATICS

The inverse kinematic problem is to calculate the joint angles for a given end point position with respect to the global coordinate frame. The closed-form of inverse kinematics of the proposed arm derived using the standard method [6,20]. The joint angles for the given end point position can be determined using the following equations:

$$\theta_1 = \text{atan2}(P_y, P_x) - \text{atan2}([L_3 - L_5]\sin\theta_3, \pm\sqrt{P_x^2 + P_y^2 - [L_3 - L_5]^2\sin^2\theta_3}) \quad (8)$$

$$\theta_2 = \sin^{-1}\left(\frac{P_z}{[L_2 - g] + [L_3 - L_5]\cos\theta_3}\right) \quad (9)$$

$$\theta_3 = \cos^{-1}\left(\frac{P_x^2 + P_y^2 + P_z^2 - (L_2-g)^2 - (L_3-L_5)^2}{2[L_2 - g][L_3 - L_5]}\right) \quad (10)$$

## DYNAMICS

The closed-form dynamic equations have been derived for the purpose of controller design. The dynamic behavior of the arm can be presented by the following equation [5,17]

$$M(\theta)\ddot{\theta} + CE(\theta)[\dot{\theta}^2] + CO(\theta)[\dot{\theta}\dot{\theta}] + G(\theta) = \tau \quad (11)$$

Where:

| | |
|---|---|
| $\tau = [\tau_1\ \tau_2\ \tau_3]^T$ | 3×1 vector of the motor torques, |
| $M(\theta)$ | 3×3 definite inertia matrix, |
| $CE(\theta)$ | 3×3 centrifugal coefficients matrix, |
| $CO(\theta)$ | 3×3 Coriolis coefficients matrix, |
| $G(\theta)$ | 3×1 vector of gravity force, |
| $\ddot{\theta}$ | $[\ddot{\theta}_1\ \ddot{\theta}_2\ \ddot{\theta}_3]^T$ |
| $[\dot{\theta}\dot{\theta}]$ | $[\dot{\theta}_1\dot{\theta}_2\ \ \dot{\theta}_1\dot{\theta}_3\ \ \dot{\theta}_2\dot{\theta}_3]^T$ |
| $[\dot{\theta}^2]$ | $[\dot{\theta}_1^2\ \ \dot{\theta}_2^2\ \ \dot{\theta}_3^2]^T$ |

$$M(\theta) = \begin{bmatrix} M_{11} & M_{12} & M_{13} \\ M_{12} & M_{22} & 0 \\ M_{13} & 0 & M_{33} \end{bmatrix}, \quad CE(\theta) = \begin{bmatrix} 0 & CE_{12} & CE_{13} \\ CE_{21} & 0 & 0 \\ CE_{31} & CE_{32} & 0 \end{bmatrix}$$

$$CO(\theta) = \begin{bmatrix} CO_{11} & CO_{12} & CO_{13} \\ 0 & CO_{22} & CO_{23} \\ CO_{31} & 0 & 0 \end{bmatrix}, \quad G(\theta) = \begin{bmatrix} 0 \\ 0 \\ 0 \end{bmatrix}$$

$$M_{11} = I_{z1} + C_2^2[I_{e1} + I_{e6} + I_{e2} + 2C_3I_{e3} + I_{y2} + m_2\bar{X}_2^2] + S_2^2[S_3^2(I_{e1} + I_{e5}) + C_3^2 I_{e4} + I_{x2}]$$

$$M_{12} = S_2S_3[I_{e3} + C_3[I_{e1} + I_{e5} - I_{e4}]]$$

$$M_{13} = C_2[I_{e1} + I_{e6} + C_3I_{e3}]$$

$$M_{22} = I_{z2} + m_2\bar{X}_2^2 + C_3^2(I_{e1} + I_{e5}) + S_3^2I_{e4} + I_{e2} + 2C_3I_{e3}$$

$$M_{33} = I_{e1} + I_{e6}$$

$$CE_{12} = C_2S_3[I_{e3} + C_3[I_{e1} + I_{e5} - I_{e4}]]$$

$$CE_{13} = -C_2S_3I_{e3}$$

$$CE_{21} = S_2C_2[\, I_{y2} - I_{x2} + m_2\bar{x}_2^2 - S_3^2 I_{e5} + C_3^2(\, I_{e1} - I_{e4}) + I_{e2} + I_{e6} + 2C_3 I_{e3}$$

$$CE_{31} = S_3[\, C_2^2 I_{e3} - S_2^2 C_3[\, I_{e1} + I_{e5} - I_{e4}\,]]$$

$$CE_{32} = S_3[\, I_{e3} + C_3[\, I_{e1} + I_{e5} - I_{e4}\,]]$$

$$CO_{11} = -2CE_{21}$$

$$2CE_{31}$$

$$CO_{13} = -S_2[\, 2S_3^2 I_{e1} + I_{e6} + \cos 2\theta_3\,[\, I_{e4} - I_{e5}\,]]$$

$$CO_{22} = S_2[\, 2C_3^2 I_{e1} + I_{e6} + 2C_3 I_{e3} - \cos 2\theta_3 \; I_{e4} \quad I_{e5}]]$$

$$CO_{23} = -2CE_{32}$$

$$-S_2[\, I_{e1} + \cos 2\theta_3\,[\, I_{e1} + I_{e5} - I_{e4}] + I_{e6} + 2C_3 I_{e3}]$$

where

$$I_{e1} = m_3\bar{x}_3^2 + m_4 L_5^2 + m_5\bar{x}_5^2$$

$$I_{e2} = m_3(L_2 - g)^2 + m_4(\bar{x}_4 - g)^2 + m_5 g^2$$

$$I_{e3} = m_3\bar{x}_3(L_2 - g) - m_4(\bar{x}_4 - g)L_5 + m_5\bar{x}_5 g$$

$$I_{e4} = I_{x3} + I_{x4} + I_{x5}$$

$$I_{e5} = I_{y3} + I_{y4} + I_{y5}$$

$$I_{e6} = I_{z3} + I_{z4} + I_{z5}$$

$I_{xi}$, $I_{yi}$, and $I_{zi}$ are the mass moments of inertia relative to x, y, z axis at the center of mass of a link i. (motor 3 is a part of link 2). The gravity term, $G(\theta)$ becomes zero when equations (3) and (4) are satisfied in the arm. This condition holds for all possible configurations.

## HARDWARE

A schematic of the system hardware is shown in figure 5. An IBM AT microcomputer which is hosting a 4-node parallel processor is used as the main controller of this robot. The parallel processor has four nodes and a PC/AT bus interface. Each node is an independent 32-bit processor with local memory and communication links to the other nodes in the system. A high speed AD/DA converter has been used for reading the velocity signals and sending analog command signals to the servo controller unit. A parallel IO board (D/D converter) between the servo controller unit and the computer allows for reading the R/D (Resolver to Digital) converter.

The servo controller unit produces three phase, Pulse Width Modulated (PWM), sinusoidal currents for the power amplifier. The servo controller unit contains an interpolator, R/D converter and a communication interface for the computer. The servo controller unit can be operated in either a closed loop velocity or current (torque) control mode (the current control is used). A PWM power amplifier, which provides up to 47 Amperes of drive current from a 325 volt power supply, is used to power the motors. The main DC bus power is derived by full-wave rectifying the three phase 230VAC incoming power. This yields a DC bus voltage of 325VDC

The motors used in this robot are neodymium (NdFeB) magnet AC brushless synchronous motor. Due to the high magnetic field strength (maximum energy products: 35 MGOe) of the rare earth NdFeB magnets, the motors have high torque to weight ratio. Pancake type resolvers are used as position and velocity sensors. The peak torque of motor 1 is 118 Nm, while the peak torques of motors 2 and 3 are 78 and 58 Nm respectively.

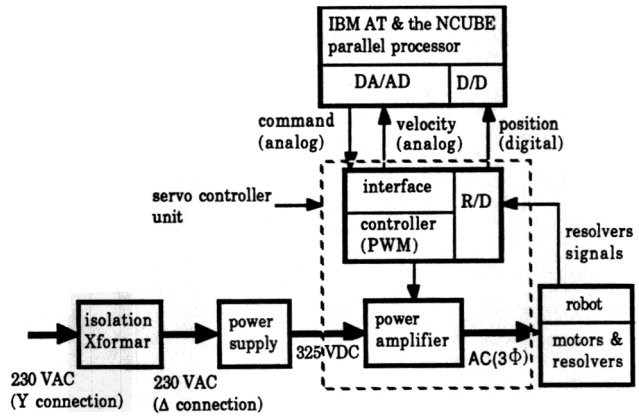


Figure 5: The control hardware for Minnesota Robot

## IDENTIFICATION OF DYNAMIC PARAMETERS

The dynamic parameters used in control were experimentally identified by a dynamic parameter identification method developed in [15]. The identification program uses the measurements of the command voltage and the joint position of the robot. The identification method can identify the inertial parameters, viscous friction, and Coulomb friction using the integrated dynamic model of the motors and links. The accuracy of the dynamic parameters was experimentally verified via the comparison of the theoretically computed trajectories and the experimental trajectories. The identified dynamic parameters for the University of Minnesota Direct Drive Robot are shown in table 1.

Table 1 Inertial parameters for the University of Minnesota Direct Drive Robot

| | Parameters | identified value | Computed value |
|---|---|---|---|
| Inertial ($kg\text{-}m^2$) | $I_{z1}$ | 0.19719 | 0.1752 |
| | $I_{x2}$ | 0.02592 | 0.04125 |
| | $m_2\bar{x}_2^2 + I_{e2} + I_{y2}$ | 1.68135 | 1.06955 |
| | $m_2\bar{x}_2^2 + I_{e2} + I_{z2}$ | 1.78135 | 1.16955 |
| | $I_{e1} + I_{e5}$ | 0.28922 | 0.298045 |
| | $I_{e1} + I_{e6}$ | 0.27759 | 0.296158 |
| | $I_{e3}$ | 0.20 | 0.2498 |
| | $I_{e4}$ | 0.14543 | 0.1319 |
| Damping in joint | motor 1 | $0.036 * \theta_1$ | |
| | motor 2 | $0.078 * \theta_2$ | |
| | motor 3 | $0.02 * \theta_3$ | |
| Coulomb in joint | motor 1 | 0.1 | |
| | motor 2 | 0.1 | |
| | motor 3 | 0.03 | |

## EXPERIMENTAL RESULTS

The preliminary evaluation of the performance of robot concerns the dynamic tracking accuracy along a specified trajectory.

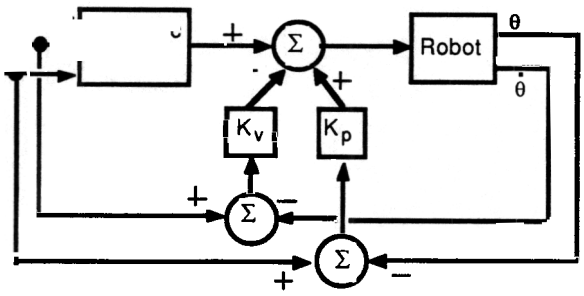


Feedforward controller

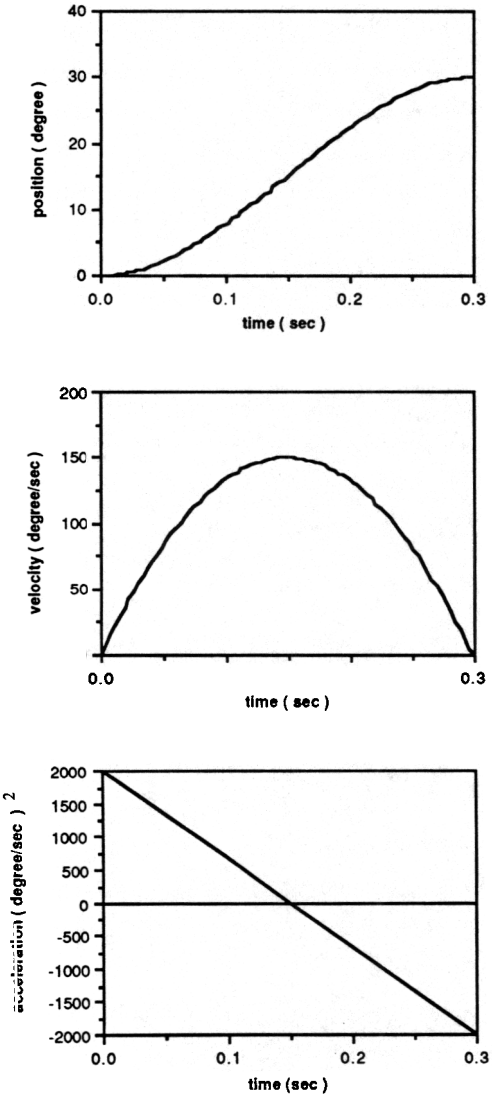


Figure 7: Position, velocity, and acceleration profiles for a cubic polynomial trajectory

A feedforward compensator, as shown in figure 6, is used to cancel the robot nonlinear terms while a set of constant gains are used in the feedback loop to decrease the error and develop robustness in modelling errors [1,3].

The reference trajectory in the experiment is generated by a cubic polynomial as shown in figure 7. The motor dynamics and the friction in the dynamic model were included. The dynamic model does not include the gravity terms because the University of Minnesota Robot is statically balanced. The robot control program, written in C language, yields a 250 Hz sampling frequency. All the joints were commanded to simultaneously move 30 degrees in 0.3 seconds from a predetermined origin. The maximum velocity and acceleration for each joint are 150 degree/sec and 2000 degree/sec$^2$, respectively.

The trajectory and velocity errors for each joint are depicted in figures 8 and 9. Figure 8 shows the trajectory and velocity errors when all the robot parameters are calculated from the engineering drawings. The maximum tracking errors are 2.3°, 1.3°, and 2.3° for joint 1, 2 and 3, respectively.

Figure 9 shows the trajectory and velocity errors with the dynamic parameters identified experimentally. The trajectory and velocity errors are significantly reduced. The peak trajectory errors are 0.7°, 1.2° and 0.44° for joint 1, 2 and 3 respectively.

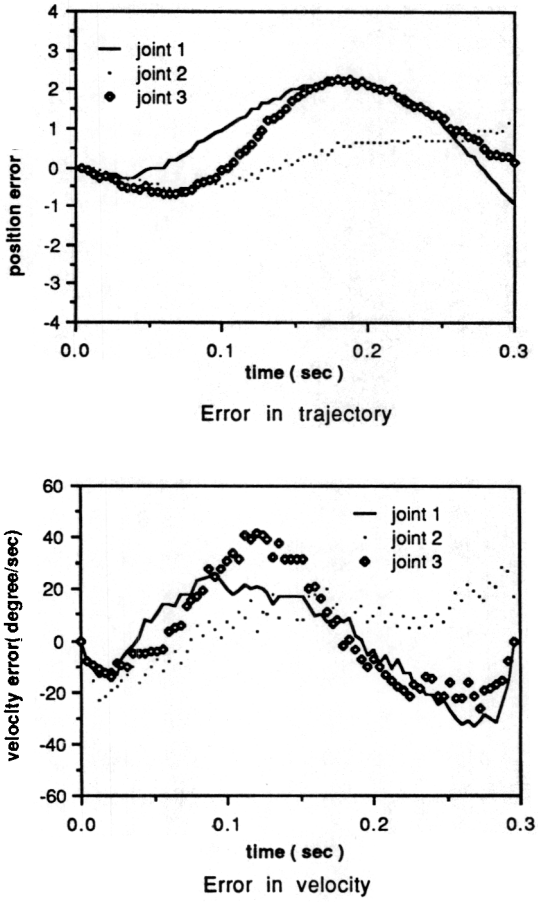


Figure 8: Trajectory and velocity error curves with the same trajectory for all three joints (All the parameters are computed from the engineering drawings)

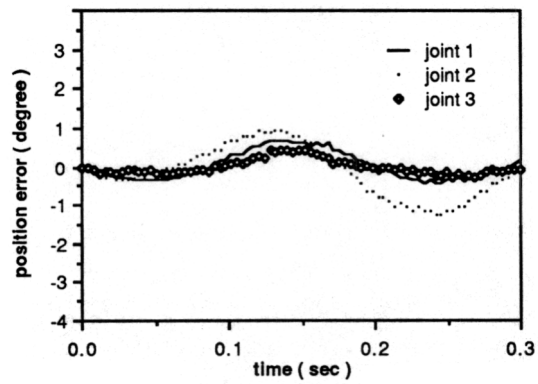


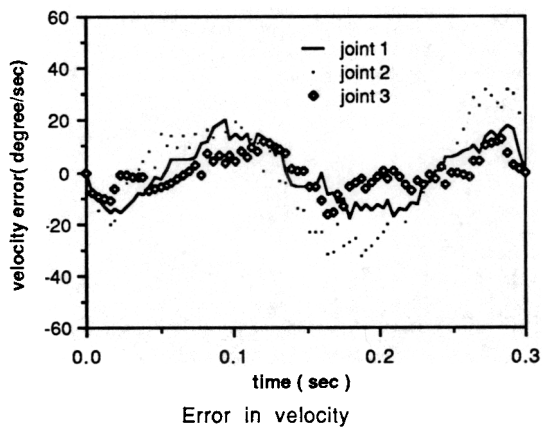


**Figure 9: Trajectory and velocity error curves with the same trajectory for all three joints. (All the parameters are experimentally identified).**

## SUMMARY

This paper presents some results of the on-going research project on statically-balanced direct drive arm at the University of Minnesota. The following features characterize this robot:

1. The statically-balanced mechanism without counter weights allows for selection of smaller actuators. Since in static or quasi-static operations, no load is on the actuators, therefore the overheating of the previous direct drive robots is alleviated.
2. The robot links are made of graphite-epoxy composite materials to give more structural stiffness and less mass. The high structural stiffness and low mass of the links allow for the wide bandwidth of the control system.
3. To improve tracking errors, the robot parameters were identified experimentally. The errors in the trajectory and velocity were reduced significantly.
4. Impedance control has been considered for control of the robot. The object of the control task is to develop a control system such that, this robot will be capable of maneuvering in constrained and unconstrained environments.

## REFERENCES

1. An, C. H., Atkeson, C. G., J. D., Hollerbach, J. M., "Experimental Determination of the Effect of Feedforward Control on Trajectory Tracking Errors", 1986 IEEE International Conference on Robotics and Automation, pp 55 - 60

2. Asada, H., Kanade, T., "Design of Direct Drive Mechanical arms", ASME Journal of Vibration, Acoustics, Stress, and Reliability in Design, vol. 105, July 1983, pp. 312 - 316

3. Asada, H., Kanade, T., and Takeyama, I., " Control of a Direct Drive Arm", Journal of Dynamic Systems, Measurements, and Control, Sept. 1983, vol. 105, pp 136 - 141

4. Asada, H. and Youcef-Toumi, K.," Analysis and Design of a Direct Drive Arm with a Five-Bar-Link Parallel Drive Mechanism ", ASME Journal of Dynamic Systems, Measurement and Control, vol. 106 No. 3, 1984, pp 225-230.

5. Asada, H. and Slotine, J.-J.E., "Robot Analysis and Control", John Wiley and Sons, 1986.

6.Craig, J. J., "Introduction to Robotics: Mechanics and Control, Addison-Wesley, Reading, Mass 1986.

7. Forrest-Barlach, M. G. and Babcock, S. M., "Inverse Dynamics Position Control of a Compliant Manipulator", IEEE 1986 International Conference on Robotics and Automation, vol 1 Apr. 1986, pp 196-205.

8. Hogan, N., "Impedance Control, An Approach Manipulation", ASME Journal of Dynamic Systems, Measurement, and Control, March, 1985.

9. Kazerooni, H., Houpt, P.K., "On the Loop Transfer Recovery", Int. Journal of Control, Vol. 43,No. 3, 1986.

10. Kazerooni, H., Sheridan, T., B., Houpt, P. K., "Fundamentals of Robust Compliant Motion for Robot Manipulators" , IEEE Journal on Robotics and Automation, vol. 2, NO. 2, June 1986.

11. Kazerooni, H., Houpt, P. K., Sheridan, T., B., " Design Method for Robust Compliant Motion for Robot Manipulators", IEEE Journal on Robotics and Automation, vol. 2, NO. 2, June 1986.

12. Kazerooni, H., "Robust Non-linear Impedance Control", In proc. of the IEEE International Conference on Robotics and Automation, Raleigh, North Carolina, April 1987.

13. Kazerooni, H., Baikovicius, J., Guo, J., "Compliant Motion Control for Robot Manipulators, Input Output Approach", In proc. of the American Control Conference, June 1987, Minneapolis.

14. Kazerooni, H., Kim, S., "Statically Balanced Direct Drive Robot for Compliance Control Analysis", presented at ASME Winter Annual Meeting, "Modeling and Control of Robotic Manipulators and Manufacturing Processes", Boston, 1987.

15. Kim, S.," Design, Analysis, and Control of a Statically Balanced Direct Drive Manipulator", Ph.D Dissertation, Dept. of Mechanical Engineering, The University of Minnesota, June 1988.

16. Kuwahara, H., One, Y., Nikaido, M. and Matsumoto, T., " A Precision Direct Drive Robot Arm", Proceedings American Control Conference, 1985, pp 722-727.

17. Luh, J. Y. S., Walker, M. W. and Paul, R. P., "Resolved - Acceleration Control of Mechanical Manipulators", IEEE Transactions on Automatic Control 25 (3) June, 1980, pp 468 - 474.

18. Mahalingam, S. and Sharan, A. M., "The Optimal Balancing of the Robotic Manipulators", IEEE 1986 International Conference on Robotics and Automation, vol. 2, Apr. 1986, pp 828-835.

19. Markiewicz, B. R., "Analysis of the Computed_Torque Drive Method and Comparision with the Conventional Position Servo for a Computer - Controlled Manipulator", Technical Memorandum 33 - 601, JPL, Pasadena, CA, March, 1973.

20. Paul, R. P.,Robot Manipulators: Mathematics, Programming, and Control", MIT press, Cambridge, Mass, 1981.

21. Rivin, E.I., "Effective Rigidity of Robot Structures: Analysis and Enhancement"', Proceedings of 85 American Control Conference, 985, 1985, pp 381-382.

22. Takase, K., Hasegawa, T. and Suehiro, T., "Design and Control of a Direct Drive Manipulator", Proceedings of the International Symposium on Design and Synthesis, Tokyo, Japan, July 1984, pp 347-352.